The Astrophysical Journal Letters, 833:L9 (5pp), 2016 December 10
doi:10.3847/2041-8213/833/1/L9

WHAT IS EATING OZONE? THERMAL REACTIONS BETWEEN SO_2 AND O_3: IMPLICATIONS FOR ICY ENVIRONMENTS

Mark J. Loeffler and Reggie L. Hudson
NASA Goddard Space Flight Center, Astrochemistry Laboratory, Code 691, Greenbelt, MD 20771, USA; mark.loeffler@nasa.gov
Received 2016 October 17; revised 2016 November 15; accepted 2016 November 15; published 2016 December 5

ABSTRACT

Laboratory studies are presented, showing for the first time that thermally driven reactions in solid $H_2O + SO_2 + O_3$ mixtures can occur below 150 K, with the main sulfur-containing product being bisulfate (HSO_4^-). Using a technique not previously applied to the low-temperature kinetics of either interstellar or solar-system ice analogs, we estimate an activation energy of 32 kJ mol^{-1} for HSO_4^- formation. These results show that at the temperatures of the Jovian satellites, SO_2 and O_3 will efficiently react making detection of these molecules in the same vicinity unlikely. Our results also explain why O_3 has not been detected on Callisto and why the SO_2 concentration on Callisto appears to be highest on that world's leading hemisphere. Furthermore, our results predict that the SO_2 concentration on Ganymede will be lowest in the trailing hemisphere, where the concentration of O_3 is the highest. Our work suggests that thermal reactions in ices play a much more important role in surface and sub-surface chemistry than generally appreciated, possibly explaining the low abundance of sulfur-containing molecules and the lack of ozone observed in comets and interstellar ices.

Key words: astrochemistry – comets: general – evolution – methods: laboratory: solid state – planets and satellites: surfaces – radiation mechanisms: thermal

1. INTRODUCTION

It is well known that ionizing radiation incident on the Jovian satellites can induce chemical changes in surface ices, but the role of low-temperature thermally induced chemistry has rarely been explored. In recent years, we have investigated bisulfite (HSO_3^-) formation from the reaction of SO_2 with H_2O at ~70 – 130 K (Loeffler & Hudson 2010), with a subsequent conversion to sulfate (SO_4^{2-}) in the presence of radiolytically generated H_2O_2 (Loeffler & Hudson 2013). However, the possibility that similar reactions might occur with other oxidants, on icy satellites, or in cometary or interstellar ices has yet to be addressed and answered. Here, we describe a second case of thermally induced oxidation, with ozone (O_3) instead of H_2O_2 as the oxidizing agent. We use this discovery to argue that thermal reactions can help explain both the observed hemispherical compositional differences on icy satellites and the lack of O_3 detections in comets and interstellar ices. We conclude (1) that such reactions in ices can play a much more important role in surface and sub-surface chemistry than is generally appreciated, and (2) that they might help resolve the discrepancy between the ease with which O_3 is made in laboratory cosmic-ice analogs and the rarity with which it is observed in interstellar and planetary environments.

The detection of ozone (O_3) on Ganymede, Rhea, and Dione (Noll et al. 1997), through the ozone's strong uv absorption near 260 nm, shows that radiation chemistry alters the composition of the surface of each of these worlds. Given that these surfaces are composed predominately of H_2O-ice, from which ozone can be produced from the O_2 made by radiolysis of H_2O, it is somewhat surprising that other icy satellites have not shown evidence of solid O_3. While there are environmental differences among icy satellites, none readily explain why Ganymede, Rhea, and Dione are the only objects where solid ozone is present.

Noll et al. (1997) noted that one reason for the lack of additional O_3 detections is that other molecules, such as SO_2, might compete for O atoms produced via radiolysis of the surface H_2O-ice. This possible anti-correlation between two molecules, SO_2 and O_3, is similar to what has been observed on Europa, where SO_2 and H_2O_2, another product of H_2O radiolysis, are largely confined to different hemispheres (Domingue & Lane 1998; Carlson et al. 1999; Hendrix et al. 2011). Through laboratory studies, our group showed that under relevant Europa conditions, SO_2 and H_2O_2 indeed react via thermally driven reactions on very short timescales (Loeffler & Hudson 2013), supporting previous observations and suggesting that at the temperatures of the icy satellites, these two molecules will not be found in the same vicinity. Furthermore, our observation that such reactions readily occur at temperatures of the icy satellites (~100 K) without the need of an external energy source underscores the importance of non-radiolytic reactions for not only surface-ice chemistry, but also for processing sub-surface ices.

Given the propensity of SO_2 to react in $H_2O + H_2O_2$ ices, we now report that thermally driven reactions also occur in $H_2O + SO_2 + O_3$ ices. In the following, we describe how infrared (IR) spectroscopy was used to both identify the main reaction products and to estimate the reaction's activation energy.

2. EXPERIMENTAL

The experimental setup, equipment, and procedures to prepare our ices and to quantify our results have been described previously (Loeffler & Hudson 2010, 2013). To make pure O_3 we filled a glass manifold with ~100 Torr of O_2 and sparked it with a Tesla coil discharge for ~15 minutes. During this time, part of the manifold was immersed in liquid nitrogen to collect the O_3 product. After the discharge was turned off, the remaining O_2 was pumped away, leaving the liquid O_3 behind.

The $H_2O + SO_2 + O_3$ (76:21:3) ices used in this study had a thickness of 1.4 ± 0.1 μm, assuming that the density of O_3 is 1.73 g cm^{-3} (Streng & Grosse 1959) and the refractive index at

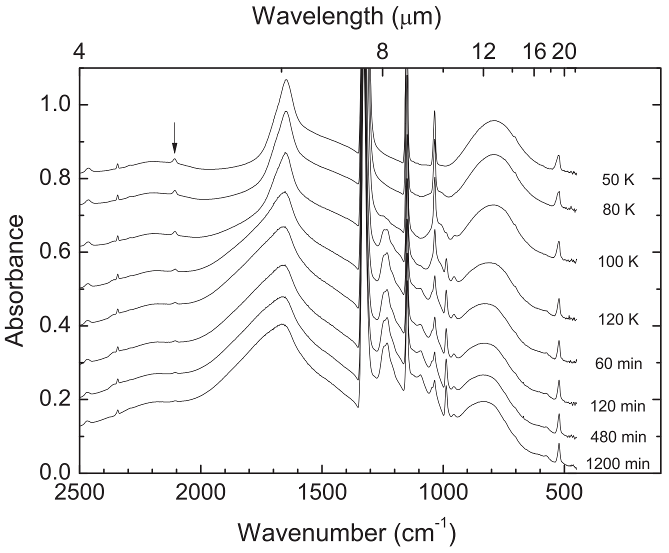

Figure 1. Evolution of a $H_2O + SO_2 + O_3$ sample (76:21:3) during heating to and annealing at 120 K. The bottom four spectra are labeled by the time elapsed after the sample had reached 120 K. The vertical arrow highlights the 2108 cm^{-1} O_3 band used for analysis.

670 nm is 1.50. We estimated the refractive index by applying the Lorentz–Lorenz approximation (Lorentz 1880; Lorenz 1881) using the published values for density and molar refractivity (Maryott and Buckley 1953). As we have done previously, we characterized our samples using infrared spectroscopy; details can be found in Loeffler & Hudson (2013).

To quantify the loss of ozone in our samples, we matched the baseline of ozone's 2108 cm^{-1} overtone absorption with a straight line and then integrated this same O_3 IR feature; we did not integrate the fundamental vibrational band at 1040 cm^{-1} because multiple products absorbed in this region, complicating the analysis. As both pure O_3 and pure SO_2 sublimate at the higher temperatures used in this study, we performed control experiments to check the possibility of thermal loss contributing to the absorption. We found that a low concentration of O_3 was thermally stable overnight in a $H_2O + O_3$ sample at 130 K. Furthermore, we also observed that between 50 and 130 K, the strength of the 2108 cm^{-1} ozone absorption band decreased nearly linearly by ∼15%, an observation we used in our calculations.

3. RESULTS

The IR spectra of an $H_2O + SO_2 + O_3$ (76:21:3) ice made by co-deposition of its components at 50 K, during warming to 120 K at 1 K $minute^{-1}$, and while holding at 120 K are shown in Figure 1. After deposition, each compound was easily identified in the 2500 – 500 cm^{-1} spectral region: O_3 (1035 and 2108 cm^{-1}), H_2O (1648 and 790 cm^{-1}), and SO_2 (2463, 1318, 1149, and 523 cm^{-1}). On warming to 80 K, spectral changes included the appearance of a new absorption at 954 cm^{-1}, the appearance of a broad shoulder under the main ozone absorption (∼1047 cm^{-1}), and a broadening on the high-wavenumber side of the H_2O band at 1649 cm^{-1}. By ∼100 K, the O_3 absorption began to decrease, which coincided with the growth of several new bands. The first identifiable new band was centered near 1230 cm^{-1}, with some structure to indicate that it might be a combination of multiple absorptions. Seemingly corresponding to the growth of the 1230 cm^{-1} feature were other, slightly weaker, absorptions at 573, 987, and 1090 cm^{-1}, which also continued to grow as the temperature increased.

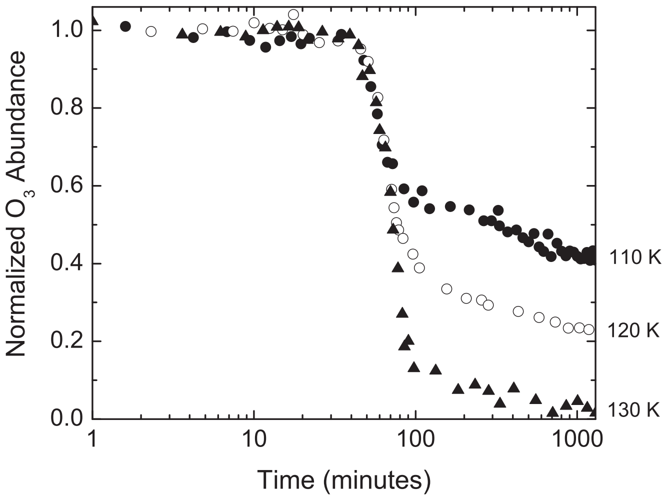

Figure 2. Decrease in the area of the 2108 cm^{-1} absorption band in a $H_2O + SO_2 + O_3$ sample (76:21:3) during heating and holding at 110, 120, and 130 K. All samples were deposited at 50 K and warmed at 1 K $minute^{-1}$.

Figure 2 shows the O_3 abundance in the sample on warming to and holding at 110, 120, and 130 K. In each experiment, the O_3 abundance started to decrease near 100 K and continued decreasing as the sample was held at a constant temperature. For the samples at 110 and 120 K, the O_3 abundance fell by a factor of 2.5 and a factor of 5.0 after 1200 minutes, while it decreased by a factor of 10 in ∼20 minutes when the sample was held at 130 K.

4. DISCUSSION

4.1. Reaction Chemistry and Spectral Assignments

To identify the likely reaction sequence observed in our experiments, one can look into work focused on thermal reactions between SO_2 and O_3 under conditions relevant to Earth's atmosphere (Erickson et al. 1977; Hoffmann 1986; Penkett et al. 1979). In those studies, the reaction sequence is thought to begin with the formation of HSO_3^- via

$$2H_2O + SO_2 \rightarrow HSO_3^- + H_3O^+. \qquad (1)$$

In samples where the bisulfate concentration is sufficiently high, $S_2O_5^{2-}$ can form through

$$2HSO_3^- \rightarrow S_2O_5^{2-} + H_2O. \qquad (2)$$

These thermal reactions are evident in the first few spectra shown in Figure 1 for our $H_2O + SO_2 + O_3$ ices. For instance, the broad shoulder near 1047 cm^{-1} is due to HSO_3^-, the absorption band at 954 cm^{-1} is from $S_2O_5^{2-}$, and the broadening of the H_2O absorption at 1648 cm^{-1} is indicative of H_3O^+.

Studies of SO_2 and O_3 in aqueous solutions found that the bisulfite from (1) was rapidly oxidized to form the bisulfate (HSO_4^-) ion (Erickson et al. 1977):

$$O_3 + HSO_3^- \rightarrow HSO_4^- + O_2. \qquad (3)$$

Figure 1 shows evidence of reaction (3) beginning near 100 K and continuing as the temperature increased, where the loss of

O_3 coincided with an increase in the large absorption band near 1230 cm^{-1}, as well as smaller ones at 1090, 987, and 573 cm^{-1}, all of which are attributed to bisulfate. We point out that the absorption near 1230 cm^{-1}, as well as the weaker one at 1090 cm^{-1}, are shifted by ~40 cm^{-1} compared to absorptions in room temperature aqueous solutions of 80 wt% H_2SO_4 (Walrafen & Dodd 1961), yet given the difference in environment this size of shift is not unreasonable. That the 1090 and 987 cm^{-1} absorptions could be from another ion, such as sulfate, which absorbs near each of these bands (Loeffler & Hudson 2013), seems unlikely given reaction (3) and that the band near 987 cm^{-1} should be much weaker than the 1090 cm^{-1} sulfate absorption, but yet it is comparable or even stronger in this ice's spectrum. Furthermore, although our sample is an amorphous solid, the 987 and 573 cm^{-1} absorptions also are observed in IR spectra of sulfuric acid monohydrate (Loeffler et al. 2011), a crystalline solid made of H_3O^+ and HSO_4^- (Taesler & Olovsson 1968).

4.2. *Kinetics*

As indicated in Figures 1 and 2, it is clear that a reaction consuming O_3 occurred in our $H_2O + SO_2 + O_3$ ice and that more O_3 was consumed as the temperature was increased. Although this temperature range over which O_3 reacted is also found on the Jovian icy satellites, it is of interest to estimate how fast this reaction will occur at lower temperatures where it cannot readily be studied on laboratory timescales. Such estimates require the reaction's activation energy, yet measuring this quantity accurately for solids is typically much more difficult than for gas- or liquid-phase solutions because of the severely limited motion in solid solutions and the distribution in alignments of potential reactants in amorphous solids, such as our ices. Nonetheless, starting with the assumption of a single-step reaction, we write

$$\frac{d\alpha}{dt} = k(T) f(\alpha), \tag{4}$$

where α is the fraction of O_3 reacted in time t, $k(T)$ is the reaction's rate constant at temperature T, and $f(\alpha)$ is the reaction model (Vyazovkin 1996). The main uncertainty in this approach is the selection of $f(\alpha)$, as the estimated activation energy can depend substantially on the selected model (see review by Vyazovkin & Wight 1997). As an alternative to this procedure, we adopt an approach known as the isoconversional method (Vyazovkin 1996), which allows one to calculate an activation energy without relying on $f(\alpha)$. Instead of the usual monitoring of a reaction at temperature T, this approach involves following a reaction subjected to a specific warming rate. We believe that this is the first time this method has been used to study the low-temperature kinetics of either interstellar or solar-system ice analogs.

To use the isoconversional method, we first rewrite (4) as

$$\frac{d\alpha}{dT} = \left(\frac{A}{\beta}\right) e^{-E/RT} f(\alpha), \tag{5}$$

where β is the heating rate, E is the reaction's activation energy, and A is the usual pre-exponential factor. Next, we take the natural log of both sides and add the subscripts α and i to the relevant dependent terms:

$$\ln\left[\beta_i \left(\frac{d\alpha}{dT}\right)_{\alpha,i}\right] = \ln\left[A_\alpha f(\alpha)\right] - E_\alpha / RT_{\alpha,i}. \tag{6}$$

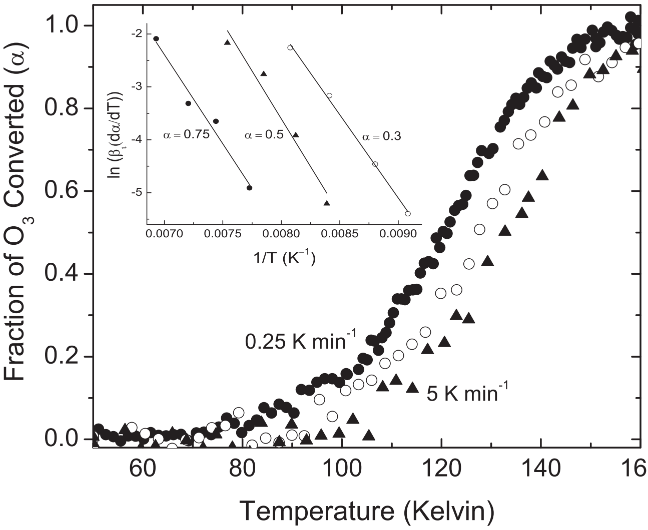

Figure 3. Fraction of O_3 converted vs. temperature for three different heating rates (K $minute^{-1}$): 0.25 (●), 2.5 (○), and 5 (▲). Inset: three fractions (0.3, 0.5, and 0.75) where Equation (6) was used to calculate the activation energy.

To use (6), we performed experiments at different heating rates (β_i) between 0.25 and 5 K $minute^{-1}$; three such experiments are shown in Figure 3, where we have plotted α as a function of temperature in the main panel. As in Figure 2, there is little to no change in the O_3 abundance below 80 K. However, for the lowest heating rates α begins to change between 80 and 100 K. In all cases, the rate of conversion increases above 100 K and more than 90% of the O_3 is converted between 140 and 150 K, depending on the heating rate. Finally, we note that the trend above ~80 K observed in Figure 3 is that the fraction (α) of O_3 consumed is largest for the slowest heating rate, a reflection of the fact that a slow heating rate translates into a longer reaction time.

To obtain an activation energy, we measured both $\frac{d\alpha}{dT}$ and $\frac{1}{T}$ at a single α for each of the curves shown in Figure 3, in a manner similar to that described by Ozawa (1965) and Flynn & Wall (1966). We estimated $\frac{d\alpha}{dT}$ by applying a linear fit to the data in close proximity to the α value in question. The inset of Figure 3 shows a plot of the left side of (6) versus $\frac{1}{T}$ for the cases of $\alpha = 0.3$, 0.5, and 0.75, with the slope of each line corresponding to $\frac{-E_\alpha}{R}$. Although it is possible that the activation energy is lower in the initial part of the reaction, we estimate E_α to be 32 ± 5 kJ mol^{-1} for $0.3 \leqslant \alpha \leqslant 0.8$, where the error given is obtained from the uncertainty of the linear fit used to determine $\frac{-E_\alpha}{R}$. This value is somewhat lower than that for reactions involving $H_2O + SO_2 + H_2O_2$ chemistry (53 kJ mol^{-1}), although a simpler approach was used there to determine the activation energy (Loeffler & Hudson 2013). The activation energy reported by Hoffmann (1986) for the $O_3 + HSO_3^-$ reaction in aqueous solution near room temperature is 46 kJ mol^{-1}, which is higher than what we measured in our ices. However, given the substantial differences in our conditions and his, we cannot say much more about these two sets of data, except that $E_\alpha = 32 \pm 5\,\mathrm{kJ\,mol^{-1}}$ appears reasonable.

One goal of kinetic analysis is to enable the extrapolation of laboratory data to estimate reaction times at temperatures where laboratory experiments are not feasible. As with deriving an activation energy, these extrapolations become much less certain as one moves away from the temperatures of the laboratory measurements. For isoconversional methods, one can calculate the time that a certain amount of material would take to react at another temperature using

$$t_\alpha = \left[\beta e^{-\frac{E_\alpha}{RT_0}}\right]^{-1} \int_0^{T_\alpha} e^{-\frac{E_\alpha}{RT}} dT, \tag{7}$$

where T_α is the temperature where α is reached at the specified heating rate and T_0 is the temperature to which one is extrapolating (Vyazovkin 1996). Estimates with Equation (7) in the present case give ~200 years for half of the O_3 in our ice to be consumed at 80 K and about 5500 years for 80% of the ozone to be converted into bisulfate. In the higher temperature regions of the icy satellites, O_3 would be consumed much more rapidly. For instance, one can use Equation (7) to estimate that 80% of the ozone would be converted in less than a minute, which is roughly consistent with our laboratory studies. These times are much shorter than what is needed to produce an observable amount of either SO_2, considering the S^+ flux irradiating the Galilean icy-satellite surfaces (Cooper et al. 2001), or O_3, based on estimates of the time to reach equilibrium via radiolysis with heavy ions at the warmer temperatures of Ganymede (Noll et al. 1996).

4.3. Implications for Ice Chemistry

Our experiments show that the O_3 abundance on any H_2O-rich icy satellite will depend on the SO_2 abundance, and vice versa. These results may be particularly relevant for Ganymede, Callisto, and Europa, where solid ozone, or its likely precursor solid O_2, and sulfur compounds are suspected to be mixed in surface ices. Thus, below we discuss observations of these icy satellites in light of our new results.

Ganymede's O_3 abundance is greatest on its trailing side (Noll et al. 1996), which is consistent with observations there of condensed O_2 (Spencer et al. 1995; Calvin et al. 1996) and with the preferential bombardment by magnetospheric ions (Johnson et al. 2004). SO_2 has been identified on Ganymede through its 4.05 μm ($2469\,\mathrm{cm^{-1}}$) absorption band (McCord et al. 1998a) but there is little information on whether SO_2 is uniformly distributed, likely due to the low abundance observed. Our results suggest that SO_2 will be more abundant on the leading hemisphere if it is mixed with the H_2O-ice. It is noted that one study observed a possible spectral feature at 320 nm, which was attributed to SO_2 frost, rather than SO_2 mixed in H_2O (Domingue et al. 1998). This feature was transient in the trailing hemisphere, but absent in the leading hemisphere. As H_2O is required to form the bisulfite that reacts with the O_3 in reaction (3), pure SO_2 frost could remain stable on an icy satellite's surface.

No O_3 has been detected on Callisto, although condensed O_2 has been identified in the trailing hemisphere (Spencer & Calvin 2002). This observation is counter to what is expected based on laboratory studies showing O_3 is easily formed from radiolysis of solid O_2 (Lacombe et al. 1997; Baragiola et al. 1999; Famá et al. 2002). Equally puzzling is the observation that SO_2 appears to be more abundant on the leading side of Callisto (McCord et al. 1998b; Hibbitts et al. 2000), which is opposite of what would be expected if SO_2 was created by magnetospheric bombardment. We note that there are alternatives to the SO_2 assignment on Callisto, such as H_2CO_3 or other carbonates (Johnson et al. 2004). However, in light of our laboratory results, it is plausible that both the lack of detection of O_3 and lower abundance of SO_2 in the Callisto's trailing hemisphere are a result of reaction (3).

On Europa, O_2 is present on both hemispheres (Spencer & Calvin 2002), yet no O_3 has been detected on either. The presence of O_3 on the trailing side is not expected given that SO_2 appears to be largely confined to this region (Lane et al. 1981; Domingue & Lane 1998; Hansen & McCord 2008; Hendrix & Johnson 2008; Hendrix et al. 2011). However, the absence of O_3 on the leading hemisphere, where SO_2 is not nearly as prevalent and even possibly absent (Hendrix et al. 2011), suggests that another compound may react with the ozone or that another process limiting production of ozone may be important.

Although our experiments were designed to probe icy-satellite chemistry, extensions to cometary and interstellar ices are possible. For example, the *Rosetta* mission's ROSINA-DFMS mass spectrometer detected O_2 at the level of about 4% relative to H_2O in the coma of comet 67P/Churyumov–Gerasimenko (Bieler et al. 2015), but no O_3 was found. Sulfur dioxide (SO_2) is a known cometary molecule and will react with H_2O-ice to make HSO_3^-, and the latter's low-temperature reaction with O_3 will lower the abundance of both HSO_3^- and O_3. If such reactions do not occur before a comet's passage around the Sun, then they will take place during it, when nuclear ices are warmed and coma material released. A second possible application of the results presented here concerns interstellar ices and their laboratory counterparts. Both radiolysis and photolysis of interstellar-ice analogs containing CO_2 readily produce detectable O_3. However, O_3 has not yet been found in the IR spectra of interstellar ices. The reason for this non-detection could be, again, that ozone's abundance is lowered by reaction of O_3 with HSO_3^-, the latter being made by the slow reaction of H_2O with SO_2 in interstellar ice-grain mantles. These reactions might also help to explain the low abundance of sulfur-containing molecules observed in interstellar ices since the expected sulfur oxyanion products have their strongest IR features in a region obscured by interstellar silicates, near $\lambda = 10\,\mu$m. We have not yet explored these possibilities.

5. CONCLUSIONS

Here, we have shown that the $H_2O + SO_2 + O_3$ reaction occurs on laboratory timescales at temperatures relevant to Ganymede, Callisto, and Europa. Therefore, this reaction may explain the lack of an O_3 detection on Callisto, as well as ozone's spatial distribution of SO_2. The detection of O_3 on the trailing side of Ganymede, also suggests that SO_2 would more likely be found on that world's leading hemisphere, yet future measurements on the spatial distribution are needed to confirm this. In addition to the icy satellites, our new results may also have implications for comets and interstellar ices, where the abundance of sulfur-containing molecules is lower than expected and ozone has yet to be detected.

In the future, we will determine the reactivity of O_3 with other molecules under relevant conditions as we have done for H_2O_2 (Loeffler & Hudson 2015). Such reactions could provide a viable explanation for why O_3 has not been detected on more icy objects. Finally, we point out that the types of reactions presented here will not necessarily be confined to icy surfaces but could also take place in sub-surface regions, serving as a thermally driven source of both O_2 and HSO_4^- for the Jovian icy satellites and other objects.

This work was supported by NASA's Outer Planets Research Program and the NASA Astrobiology Institute's Goddard Center for Astrobiology.

REFERENCES

Baragiola, R. A., Atteberry, C. L., Bahr, D. A., et al. 1999, NIMPB, 157, 233
Bieler, A., Altwegg, K., Balsiger, H., et al. 2015, Natur, 526, 678
Calvin, W. M., Johnson, R. E., & Spencer, J. R. 1996, GeoRL, 23, 673
Carlson, R. W., Anderson, M. S., Johnson, R. E., et al. 1999, Sci, 283, 2062
Cooper, J. F., Johnson, R. E., Mauk, B. H., Garrett, H. B., & Gehrels, N. 2001, Icar, 149, 133
Domingue, D. L., & Lane, A. L. 1998, GeoRL, 25, 4421
Domingue, D. L., Lane, A. L., & Beyer, R. A. 1998, GeoRL, 25, 3117
Erickson, R. E., Yates, L. M., Clark, R. L., et al. 1977, AtmEn (1967), 11, 813
Famá, M., Bahr, D. A., Teolis, B. D., et al. 2002, NIMPB, 193, 775
Flynn, J. H., & Wall, L. A. 1966, JPoSL, 4, 323
Hansen, G. B., & McCord, T. 2008, GeoRL, 35, L01202
Hendrix, A. R., Cassidy, T. A., Johnson, R. E., et al. 2011, Icar, 212, 736
Hendrix, A. R., & Johnson, R. E. 2008, ApJ, 687, 706
Hibbitts, C. A., McCord, T. B., & Hansen, G. B. 2000, JGR, 105, 22541
Hoffmann, M. R. 1986, AtmEn (1967), 20, 1145
Johnson, R. E., Carlson, R. W., Cooper, J. F., et al. 2004, in Jupiter: The Planet, Satellites and Magnetosphere, ed. F. Bagenal, T. Dowling, & W. B. McKinnon (Cambridge: Cambridge Univ. Press), 485
Lacombe, S., Cemic, F., Jacobi, K., et al. 1997, PhRvL, 79, 1146
Lane, A. L., Nelson, R. M., & Matson, D. L. 1981, Natur, 292, 38
Loeffler, M. J., & Hudson, R. L. 2010, GeoRL, 37, 19201
Loeffler, M. J., & Hudson, R. L. 2013, Icar, 224, 257
Loeffler, M. J., & Hudson, R. L. 2015, AsBio, 6, 453
Loeffler, M. J., Hudson, R. L., Moore, M. H., et al. 2011, Icar, 215, 370
Lorentz, H. A. 1880, Wiedem Ann, 9, 641
Lorenz, L. 1881, Wiedem Ann, 11, 70
Maryott, A. A., & Buckley, F. 1953, Table of Dielectric Constants and Electric Dipole Moments of Substances in the Gaseous State, National Bureau of Standards Circular 537 (Gaithersburg, MD: NIST)
McCord, T. B., Hansen, G. B., Clark, R. N., et al. 1998a, JGR, 103, 8603
McCord, T. B., Hansen, G. B., Fanale, F. P., et al. 1998b, Sci, 280, 1242
Noll, K. S., Johnson, R. E., Lane, A. L., et al. 1996, Sci, 273, 341
Noll, K. S., Roush, T. L., Cruikshank, D. P., et al. 1997, Natur, 388, 45
Ozawa, T. 1965, B. Chem. Soc. Jpn., 38, 1881
Penkett, S. A., Jones, B. M. R., Brich, K. A., et al. 1979, AtmEn (1967), 13, 123
Spencer, J. R., & Calvin, W. M. 2002, AJ, 124, 3400
Spencer, J. R., Calvin, W. M., & Person, M. J. 1995, JGR, 100, 19049
Streng, A. G., & Grosse, A. V. 1959, JAChS, 81, 805
Taesler, I., & Olovsson, I. 1968, Acta Crystallogr., B24, 299
Vyazovkin, S. 1996, Int. J. Chem. Kinet., 28, 95
Vyazovkin, S., & Wight, C. A. 1997, ARPC, 48, 125
Walrafen, G. E., & Dodd, D. M. 1961, Trans. Faraday Soc., 57, 1286